Quasi-energies and Floquet states of two weakly coupled Bose-Einstein condensates under periodic driving

Xiaobing Luo, Qiongtao Xie, and Biao Wu
Institute of Physics, Chinese Academy of Sciences, Beijing 100080, China

We investigate the quasi-energies and Floquet states of two weakly coupled Bose-Einstein condensates driven by a periodic force. The quasi-energies and Floquet states of this system are computed within two different theoretical frameworks: the mean-field model and the second-quantized model. The mean-field approach reveals a triangular structure in the quasi-energy band. Our analysis of the corresponding Floquet states shows that this triangle signals the onset of a localization phenomenon, which can be regarded as a generalization of the well-known phenomenon called coherent destruction of tunneling. With the second quantized model, we find also a triangular structure in the quantum quasi-energy band, which is enveloped by the mean-field triangle. The close relation between these two sets of quasi-energies is further explored by a semi-classical method. With a Sommerfeld rule generalized to time-dependent systems, the quantum quasi-energies are computed by quantizing semiclassically the mean-field model and they are found to agree very well with the results obtained directly with the second-quantized model.

PACS numbers: 03.75.Kk, 03.75.Lm, 42.50.Vk, 05.30.Jp

I. INTRODUCTION

Due to its simplicity, a single particle in a double-well potential has been a paradigm to demonstrate many fundamental quantum phenomena, in particular, quantum tunneling and its control[1]. Immediately after the experimental creation of Bose-Einstein condensates (BECs) with dilute alkali atomic gases[2, 3], people realize the new possibility of putting a BEC in a double-well potential and using it to mimic this paradigm system to demonstrate experimentally quantum tunneling and other fundamental quantum phenomena. The subsequent studies show that a BEC in a double-well potential has richer physics due to interaction. For example, it was found that the tunneling of BEC between the wells can be suppressed and therefore self-trapped in one of the wells[4]-[5]. This self-trapping phenomenon has now been observed experimentally with a BEC[6, 7]. More interestingly, the nonlinear two-mode model derived to describe a BEC in a double-well potential was found to be able to describe the tunneling between Bloch bands for a BEC in an optical lattice[8]. Due to interaction, a new quantum phenomenon called nonlinear Landau-Zener tunneling was predicted and later observed in experiment[8, 9].

It is known that, for a single particle in a double-well potential, one can use an external periodically driving field to control quantum tunneling, either enhancing[10]-[12] or suppressing it[13]-[23] One then wonders whether this kind of control can be also achieved for a BEC in a double-well potential. There have been several studies in this regard[24]-[30]. These studies indeed find that the periodically driving force can strongly affect the tunneling between two weakly coupled BECs and therefore be used to control the tunneling. Recently, we found that such a control of quantum tunneling can also be achieved in an optical waveguide system[31] and be used to improve the performance of an all-optical switch[32].

In this paper we investigate the quasi-energies and Floquet states of two weakly coupled BECs under periodic driving, which can be realized experimentally with either a double-well potential or an optical lattice[33]. Quasi-energies and Floquet states are two basic concepts and tools in describing and understanding periodically driving systems. One can use either a mean-field nonlinear two-mode model or a second quantized model to describe such a system. In this paper we use both models to compute the quasi-energies and Floquet states. In the mean-field two-mode model, we discover that there can be more than two Floquet states and quasi-energies in a certain range of parameters that characterize the amplitude and frequency of the modulating force. With these additional Floquet states, there appears a triangle in the quasi-energy levels. This triangular structure in quasi-energies turns out to be crucial to understanding the localization phenomenon that has been found and studied previously[24, 25, 27]. Our analysis shows that the localization phenomenon can be regarded as a generalization of a well-known phenomenon called coherent destruction of tunneling(CDT). Therefore, we call it nonlinear coherent destruction of tunneling(NCDT)[31].

In the second quantized model, our computation also reveals a triangular structure in the quasi-energy levels. Interestingly, the quantum triangle is enveloped perfectly by the mean-field triangle, indicating a close connection between these two different approaches. By analyzing the corresponding Floquet states, we find that this quantum triangle of quasi-energies is also connected to the localization phenomenon called NCDT. The close relation between quantum quasi-energies and mean-field quasi-energies is further explored by a semi-classical method. By using a Sommerfeld quantization rule adapted for a time-dependent system, we re-calculate the quantum quasi-energies by quantizing semiclassically the mean-field model. The results match very well with the quantum quasi-energies obtained by directly using the second

quantized model.

Due to the complication brought by the chaos in the region of moderate frequencies, the focus of our paper is on cases of high frequency modulation.

II. QUASI-ENERGIES AND FLOQUET STATES

We consider a system of N identical bosons, which can occupy only two quantum states. If there is interaction between bosons, the system Hamiltonian reads[3]

$$\begin{aligned} H_q &= \frac{\gamma}{2}(\hat{a}^\dagger\hat{a}-\hat{b}^\dagger\hat{b})-\frac{v}{2}(\hat{a}^\dagger\hat{b}+\hat{a}\hat{b}^\dagger) \\ &\quad +\frac{c}{2N}(\hat{a}^\dagger\hat{a}^\dagger a\hat{a}+\hat{b}^\dagger\hat{b}^\dagger\hat{b}\hat{b})\,, \end{aligned} \tag{1}$$

where γ is the energy difference between the two quantum states denoted by $\hat{a}^\dagger, \hat{a}$ and $\hat{b}^\dagger, \hat{b}$ and v is the coupling constant between the two modes. The interaction strength is given by

$$c = \frac{4\pi\hbar^2 a_s}{m}\int |\psi_0(\vec{r})|^4 d\vec{r}\,, \tag{2}$$

where we have used a reasonable assumption that the wave functions of the two quantum states are the same except a possible trivial shift of the center and the wave function is normalized $\int|\psi_0(\vec{r})|^2 d\vec{r}=1$.

When the temperature is very low so that we can ignore any thermal effect and at the same time the number of bosons N is very large, it is appropriate to make the following coherent substitutes

$$a=\langle\hat{a}\rangle/\sqrt{N}\,,\qquad b=\langle\hat{b}\rangle/\sqrt{N}\,. \tag{3}$$

This leads to a mean-field Hamiltonian

$$\begin{aligned} H_{mf} &= \frac{\langle H_q\rangle}{N}=\frac{\gamma}{2}(|a|^2-|b|^2)-\frac{v}{2}(a^*b+ab^*) \\ &\quad +\frac{c}{2}(|a|^4+|b|^4)\,. \end{aligned} \tag{4}$$

The system described above has now been realized with a double-well potential. For the experiment in Ref.[6], there are about 1150 atoms and a simple estimate gives $v \approx 65.3\mathrm{s}^{-1}$ and $c/v \approx 15$. This system can also be realized experimentally with an optical lattice[8, 33].

In our study, we have $\gamma = A\cos(\omega t)$, that is, the energy difference between the two quantum states is changed periodically. With the double-well potential, this can be achieved by shifting periodically the power of lasers that generate the double wells. For an optical lattice, this can be accomplished by shaking along the lattice direction. We focus our study on the quasi-energies and Floquet states of this system as these are two basic concepts and tools in understanding a periodically driving system.

A. Mean-field model

We first consider the mean-field model. From the mean-field Hamiltonian (4), we can obtain a two-mode Gross-Pitaevskii equation

$$i\frac{d}{dt}\begin{pmatrix} a \\ b \end{pmatrix} = \begin{pmatrix} \frac{\gamma}{2}+c|a|^2 & -\frac{v}{2} \\ -\frac{v}{2} & -\frac{\gamma}{2}+c|b|^2 \end{pmatrix}\begin{pmatrix} a \\ b \end{pmatrix}, \tag{5}$$

where we have used the natural unit $\hbar = 1$. Although the parameters c, v, A, and ω are of unit of energy, we shall treat them as dimensionless parameters in the following discussion because what is essential is the ratios between these parameters not their absolute values.

Like its linear counterpart, a nonlinear periodic time dependent equation admits solutions in the form of Floquet states. For Eq.(5), its Floquet state has the following form

$$\begin{pmatrix} a \\ b \end{pmatrix} = e^{-i\varepsilon t}\begin{pmatrix} \phi_1(t) \\ \phi_2(t) \end{pmatrix}, \tag{6}$$

where both $\phi_1(t)$ and $\phi_2(t)$ are periodic functions of period of $T = 2\pi/\omega$ and the constant ε is the corresponding quasi-energy. After one period, this solution returns to its original state by picking up an extra phase of εT. To calculate numerically Floquet states and quasi-energies, we follow the strategy that was used to compute nonlinear Bloch states and the eigen-energies[34]. In this strategy, we expand the Floquet states in Fourier series

$$\phi_1 = \sum_{n=-L}^{L} a_n e^{in\omega t},\quad \phi_2 = \sum_{n=-L}^{L} b_n e^{in\omega t}, \tag{7}$$

where L is the cut-off and equal to 10 in our computation. With the substitution of the above Fourier series into Eq. (5), one can obtain $4L + 2$ equalities for the coefficients of each Fourier term $e^{in\omega t}$. The Floquet state and the quasi-energy are found by finding the roots of this set of $4L + 2$ nonlinear equations. Our method is different from the previous methods used to compute Floquet states and quasi-energies[24]. We believe that it is more powerful. For example, it can find the Floquet states that correspond to hyperbolic fixed points in Poincaré section, which can not be found with the previous method[24].

Our numerical results of quasi-energies are plotted in Fig.1. It is clear from Fig.1 that, for the linear case, there are two quasi-energies at a given value of A/ω with one isolated degeneracy point. For the nonlinear case, we notice that there are three quasi-energies within a certain range of A/ω with two of them degenerate. The three quasi-energies form a triangle in the quasi-energy levels as seen in Fig.1(b). Among the three quasi-energies, two quasi-energy levels are similar to their linear counterparts with one isolated degenerate point while the third quasi-energy level has no linear counterpart. Moreover, the third quasi-energy is degenerate and corresponds to two different Floquet states; this is indicated by marking the

same point in Fig.1(b) with two symbols P_1 and P_2. Note two things: (1) there is no threshold value of c for the triangle to appear; (2) the right corner of triangle is open for relatively larger nonlinear parameter c.

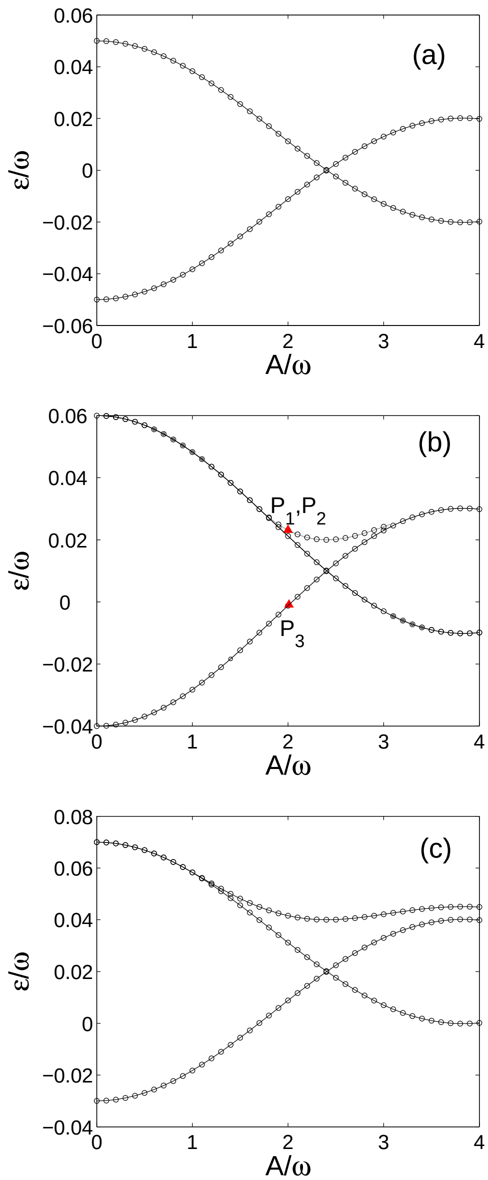

FIG. 1: (Color online)Quasi-energies as a function of A/ω at (a)$c = 0$; (b)$c = 0.4$; (c)$c = 0.8$. Solid lines are numerical results and circles are the approximate analytical results for high frequencies with Eqs.(9,10). $v = 1, \omega = 10$.

Despite the obvious similarity between the nonlinear Floquet states and the linear ones, there are a couple of conceptual differences. (1) A periodically driven n-level linear system possesses precisely n Floquet states whereas the number of nonlinear Floquet states of n-mode system can be bigger than n as we have witnessed above. (2) In linear case, all wave functions can be decomposed into a superposition of Floquet states and, therefore, the dynamics of the system is dictated by Floquet states. In the nonlinear case, the superposition principle breaks down, the dynamics of the system can no longer be completely determined by Floquet states.

The triangular structure of the quasi-energy is very similar to the energy loop discovered within the context of nonlinear Landau-Zener tunneling[8]. In fact, they are mathematically related. For high frequencies, $\omega \gg \max\{v, c\}$, we take advantage of the transformation

$$a = a' \exp[-i\frac{A\sin(\omega t)}{2\omega}], \quad b = b' \exp[i\frac{A\sin(\omega t)}{2\omega}]. \qquad (8)$$

After averaging out the high frequency terms[25, 35], we obtain a non-driving nonlinear model,

$$i\dot{a}' = -\frac{v}{2}J_0(A/\omega)b' + c|a'|^2a', \qquad (9)$$

$$i\dot{b}' = -\frac{v}{2}J_0(A/\omega)a' + c|b'|^2b', \qquad (10)$$

where J_0 is the zeroth-order Bessel function. It is clear from the transformation in Eq.(8) that the eigenstates of the above non-driving nonlinear equations correspond to the Floquet states of Eq.(5). We have computed the eigenstates of Eqs.(9,10) and the corresponding eigenenergies, which are plotted as circles in Fig.1. The consistency with our previous numerical results is obvious. As is known in Ref.[8], the above nonlinear model admits additional eigenstates when $c > J_0(A/\omega)v$. Therefore, this can be regarded as the condition for the extra Floquet states to appear for the driving nonlinear model Eq.5 at high frequencies. Since the Bessel function $J_0(A/\omega)$ can be zero, there is no threshold value of c for the triangle to appear in the quasi-energy band.

The nonlinear Floquet states are also examined thoroughly. We find that some of them are localized, which is very different from the linear Floquet states that are always unlocalized. To describe localization, we introduce a new variable, $p = (|a|^2 - |b|^2)/2$, which measures the population difference between the two modes. One Floquet state is localized if the average of p over one period,

$$\langle p \rangle_t = \frac{1}{T}\int_0^T dt\, p(t)\,, \qquad (11)$$

is nonzero; it is unlocalized if $\langle p \rangle_t = 0$. In Fig.2 , the population difference p is plotted as a function of time for three stable nonlinear Floquet states marked as P_1, P_2, P_3 in Fig.1(b). Evidently, one of these states is unlocalized since p oscillates around zero. However, two other states are localized with p oscillating around a non-zero value. The localization means that the BEC described by such Floquet states tends to stay in one mode and reluctant to tunnel to the other mode. Therefore, localization can be understood as a suppression of tunneling. Our study shows that on one hand, all the localized Floquet states correspond to the highest quasi-energies on the triangle and on the other hand, all Floquet states in the linear case and all the Floquet states not related to the quasi-energy triangle are not localized. This implies that the

triangle in Fig.1 is related to localization or suppression of tunneling. This is indeed the case as we have shown in Ref.[31]. We shall not repeat what we have done in Ref.[31]; we shall look into this connection from a different angle.

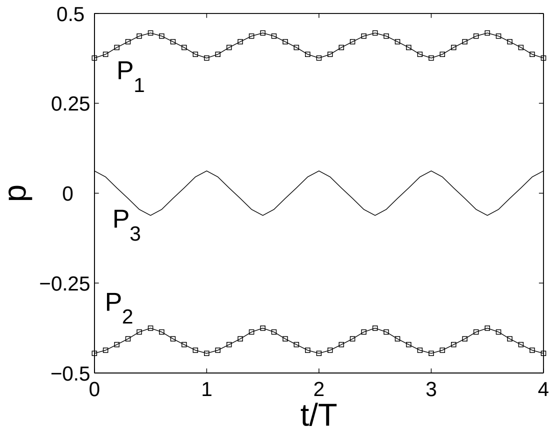

FIG. 2: Population imbalance p for three stable nonlinear Floquet states at $c = 0.4, v = 1, \omega = 10, A/\omega = 2.0$, for an interval of four periods of the driving force(solid lines). The Floquet states correspond to the quasi-energies in Fig.1(b) marked as P_1, P_2, P_3 with triangles. The squares are for Floquet states in the highest two quantum quasi-energy levels with $N = 500$.

In the mean-field model (5), the norm $|a|^2 + |b|^2 = 1$ is conserved and the overall phase is not essential to the dynamics. Therefore, we can reduce the complex dynamical variables $a = |a|e^{i\theta_a}$, $b = |b|e^{i\theta_b}$ to a pair of real variable, $p = (|a|^2 - |b|^2)/2$ and the relative phase $q = \theta_b - \theta_a$. In terms of p and q, the mean-field Hamiltonian (4) becomes

$$H_{cl} = Ap\cos(\omega t) - \frac{v}{2}\sqrt{1-4p^2}\cos q + \frac{c}{4}(4p^2+1). \quad (12)$$

As p and q are canonically conjugate variables of the above classical Hamiltonian system, one can derive a set of equations of motion. From the equations of motion, one can plot the Poincaré section of this system. Two Poincaré sections are illustrated in Fig.3 for two sets of parameters. As the overall phase is removed, the Floquet states correspond to the fixed points in Poincaré section.

The parameters for Fig.3(a) are outside the triangle range. In this figure, there are only two fixed points located at $p = 0$ and all the motions around the fixed points are oscillating around $p = 0$, indicating no localization or suppression of tunneling. The situation is different in Fig.3(b), whose parameters lie in the triangle range. In Fig.3(b), there are four fixed points: one at $q = 0$(or 2π); three at $q = \pi$. Among the three at $q = \pi$, one is hyperbolic and unstable whereas the other two are not only stable but localized. Moreover, all the orbits surrounding these two stable fixed points at $q = \pi$ are localized solutions. These again show that the triangle structure in quasi-energies are related to localization or suppression of tunneling.

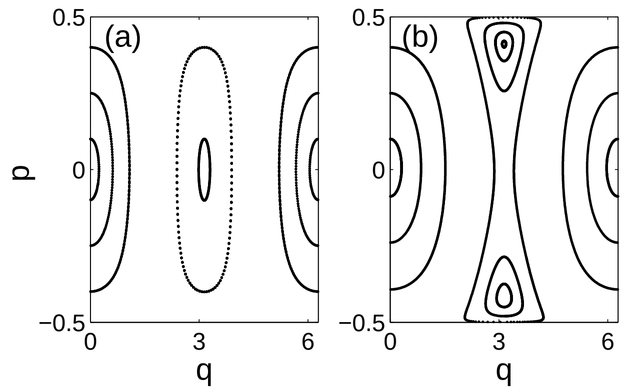

FIG. 3: Poincaré surface of section of the Hamiltonian (12). (a)$A/\omega = 0.1$; (b)$A/\omega = 2.0$. Other parameters are $c = 0.4$, $v = 1$, $\omega = 10$.

In Ref.[31], the localization phenomenon discussed above is called nonlinear coherent destruction of tunneling (NCDT). There are two reasons for this. First, the degeneracy point in Fig.1(a) is related to a localization phenomenon called coherent destruction of tunneling (CDT) and the triangle can be seen as the result of enlargement of the degenerate point by nonlinearity. Second, as we have seen in Fig.3, the localization phenomenon is intimately related to the nonlinear Floquet states and we know that CDT is related to linear Floquet states. The localization phenomenon which we call NCDT has been called in literature self-trapping or, more precisely, periodically modulated self-trapping[24, 25, 27].

B. Second quantized model

We now turn to the second quantized model (1) and compute its Floquet states and quasi-energies. For a non-driving system, it is well known that the eigen-energies and eigenstates of the second quantized model are closely connected to its mean-field counterparts[36, 37]. For this periodically driving system, we want to explore how its quantum Floquet states and quasi-energies are related to its mean-field counterparts and the localization phenomenon called NCDT.

We follow the well established Floquet theory for a quantum system[38, 39] to compute numerically quantum Floquet states and quasi-energies. In the process, we have converted the second quantized Hamiltonian (1) into a pseudo-spin Hamiltonian by introducing three angular momentum operators $\hat{J}_x = (\hat{a}^\dagger\hat{b} + \hat{b}^\dagger\hat{a})/2$, $\hat{J}_y = i(\hat{b}^\dagger\hat{a} - \hat{b}\hat{a}^\dagger)/2$, and $\hat{J}_z = (\hat{a}^\dagger\hat{a} - \hat{b}^\dagger\hat{b})/2$, for which the Casimir invariant is $\hat{J}^2 = (N/2)(N/2+1)$. The second

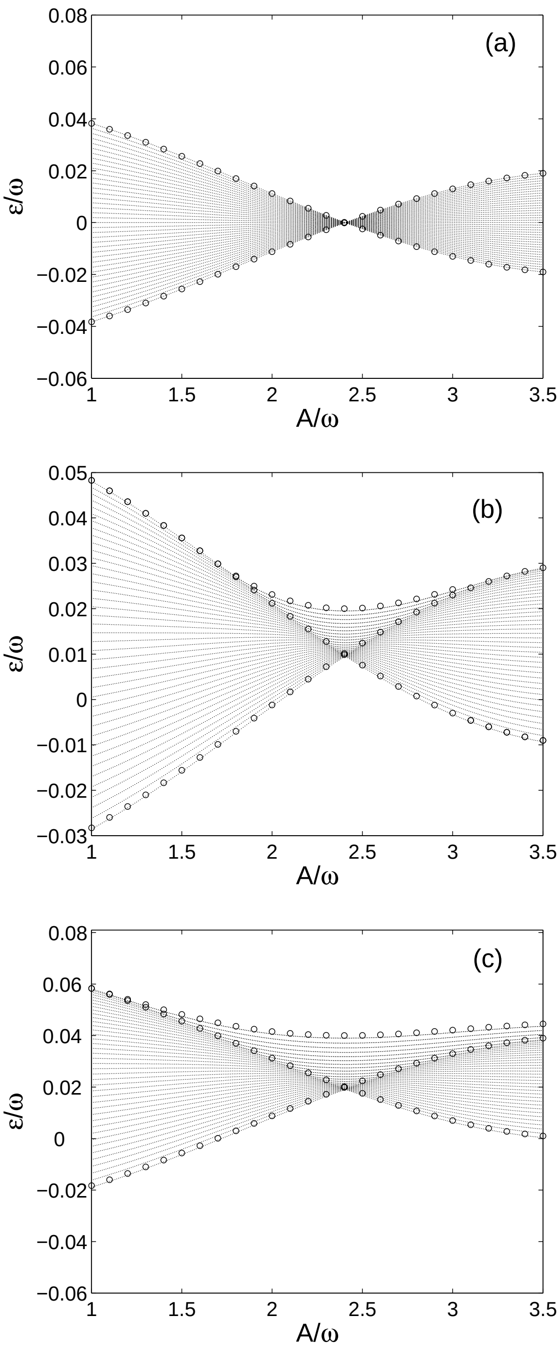

FIG. 4: Quantum quasi-energies ($N = 40$) as a function of A/ω at $v = 1, \omega = 10$ for (a) $c = 0.0$; (b)$c = 0.4$; (c)$c = 0.8$. The open circles are mean-field quasi-energies. Note that for comparison with mean-field theory, the quantum quasi-energies have been divided by N.

quantized Hamilton of the system then becomes

$$H_q = -v\hat{J}_x + \frac{c}{N}\hat{J}_z^2 + A\cos(\omega t)\hat{J}_z + \frac{c}{4}(N-2). \quad (13)$$

With this transformation, our system of N identical bosons becomes a spin system, whose Hilbert space is spanned by $N+1$ spin states $|J = N/2, J_z = M\rangle$ with $M = -N/2, -N/2+1, \cdots, N/2$.

Our numerical results for quantum quasi-energies for $N = 40$ are shown in Fig.4. We immediately notice that these quantum quasi-energy levels have very similar structures to their mean-field counterparts. For the non-interacting case in Fig.4(a), there is a single degeneracy point. For interacting cases in Fig.4(b)&(c), there are triangular structures just as in the mean-field model. For comparison, the mean-field quasi-energies are plotted as open circles in Fig.4. To one's amazement or expectation, the quantum quasi-energies are bounded by the mean-field results perfectly. Another interesting feature in Fig.4 is that all the quasi-energies in the triangle area is doubly degenerate and this degeneracy immediately breaks up outside the triangle. The feature is related the localization phenomenon NCDT as we shall discuss next.

There is also a close relation between quantum Floquet states and mean-field Floquet states. We examine this relation in terms of localization. To measure how a quantum Floquet state is localized, we define

$$\langle P\rangle_t = \frac{1}{T}\int_0^T dt\langle u_n(t)|\hat{J}_z|u_n(t)\rangle \quad (14)$$

for a given Floquet state $|u_n(t)\rangle$. This variable $\langle P\rangle_t$ quantifies the population difference between the two modes. We have plotted this variable for certain quantum Floquet states in Fig. 5. It is apparent from this figure that only the Floquet states for the quasi-energies inside the triangle are localized. This again establishes the connection of the triangle (quantum or mean-field) to the localization phenomenon NCDT. This localization also explains why the Floquet states inside the triangle are doubly degenerate. When localization occurs, there are two equal possibilities. It can localize either in mode a or in mode b; this leads to degeneracy. The mean-field results are also plotted in Fig. 5. They match very well with the results for the two highest quantum Floquet states. This good correspondence can be more clearly seen in Fig. 2, the temporal evolution of two highest quantum Floquet sates agrees very well with the mean-field results for an interval of four periods of the driving.

The quantum quasi-energies and Floquet state were studied in Ref.[24]. Their relation to the localization was also examined there. Our primary purpose here is to compare them to the mean-field results and explore their relations, which has not been studied so far.

III. SEMICLASSICAL QUANTIZATION

In the previous section, we have demonstrated by direct numerical computation how the quantum Floquet states and quasi-energies are connected to their mean-field counterparts. This relation can be further explored with a semiclassical method as the mean-field model (4)

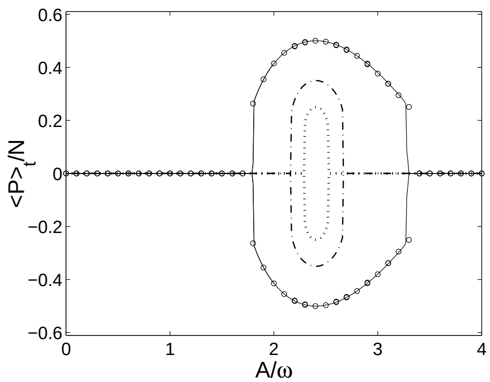

FIG. 5: Population difference $\langle P\rangle_t$ for every Floquet state in the highest two quantum quasi-energy levels(solid line), the 149th and 150th quantum quasi-energy levels(dot-dashed line), and the 249th and 250th quantum quasi-energy levels(dotted line) at $c/v = 0.4, \omega/v = 10, N = 500$. The open circles are for the population difference $\langle p\rangle_t$ for the highest mean-field quasi-energy level in Fig.1(b).

can be regarded as the classical limit of the second quantized model (1) in the limit of $N \to \infty$[40]. We shall follow the procedure in Ref. [37, 41, 42, 43] and try to quantize the classical Hamiltonian in Eq.(12), which is equivalent to Hamiltonian (4), with the Sommerfeld rule. However, as our system is time dependent, the usual Sommerfeld quantization rule has to be generalized.

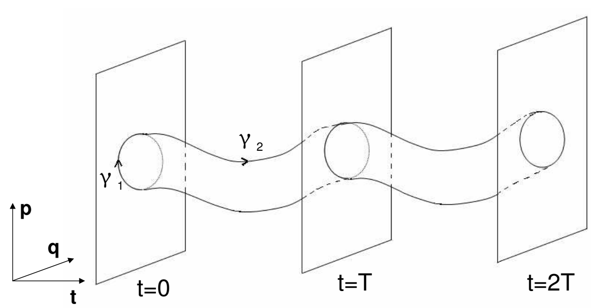

FIG. 6: Periodic vortex tube. Two paths are shown. The path γ_1 lies in a plane of t=const and γ_2 is a path connecting a point (p, q) at time t with the same point at time $t + T$.

The generalization of the Sommerfeld rule has been done for any time-dependent system[44, 45]. The basic idea is to regard time as a dynamic variable and introduce a new canonical momentum which conjugates time. We shall not go into the details of this theory and shall only describe how this generalization works for the case of our interest, a periodic time dependent system. As seen in the Poincaré section of Fig.3, there are closed orbits around fixed points. These closed orbits will change their positions and shapes in the phase space with time and return to their original points and shapes after one period. This kind of evolution forms a tube in the space spanned by p, q, t as depicted in Fig.6. This tube is called vortex tube. As the system is periodic in time, the tube in Fig.6 is essentially a torus. The quantization can be done by choosing two independent closed paths on the vortex tube which cannot be homotopically deformed onto each other and requiring

$$I_1 = \frac{1}{2\pi}\oint_{\gamma_1} pdq = n_1\hbar/N\,, \tag{15}$$

$$\begin{aligned} I_2 &= \frac{1}{2\pi}\oint_{\gamma_2}(pdq - H_{cl}dt) + \frac{T}{2\pi}\varepsilon \\ &= n_2\hbar\,, \end{aligned} \tag{16}$$

where n_1 and n_2 non-negative integers. The quantization is done in two steps: (1) we first find a path γ_1 that fulfills the quantization condition for I_1; (2) the quantization condition for I_2 is then used to compute the quasi-energy ε as

$$\varepsilon_{n_1,n_2} = -\frac{1}{T}\oint_{\gamma_2}(pdq - H_{cl}dt) + n_2\omega. \tag{17}$$

In the above, $n_2\omega$ means that quasi-energy ε is only defined modulo ω, reflecting the unique nature of quasi-energy. One can view $\hbar/N$ in Eq.(15) as the effective Plank constant[37, 41, 42], which goes to zero at the limit of $N \to \infty$.

Our semiclassical results of quasi-energies are plotted in Fig.7 to compare with the quantum quasi-energies obtained directly from the second quantized model. They match perfectly, indicating the success of the generalized Sommerfeld quantization rule. In our calculation, the path γ_1 is chosen as the closed orbit in the Poincaré section and γ_2 is the path along the maximal points of p on the tube as illustrated in Fig.6. Note that the natural unit $\hbar = 1$ is used in our calculation.

These semiclassical results are very helpful in understanding why the quantum quasi-energies are enveloped by the mean-field quasi-energies as seen in Fig.4. We first look at the simple case when there are only two fixed points in the Poincaré section, as in Fig.3(a). The fixed point at $q = 0$ corresponds to the nonlinear Floquet state with lower quasi-energy and the other fixed point corresponds to the Floquet state with higher quasi-energy. This implies that the quantization for orbits around the fixed point at $q = 0$ produces quasi-energies that are higher than the corresponding mean-field quasi-energy and the quantization for orbits around the fixed point at $q = \pi$ yields quasi-energies that are lower than the corresponding mean-field quasi-energy. As a result, the quantum quasi-energies are bounded by the mean-field quasi-energies. The double degeneracy of the quantum quasi-energies within the triangle can also be explained with this semiclassical approach. As shown in Fig.3(b), there are two stable fixed points at $q = \pi$. These two fixed points correspond to two Floquet states with the same quasi-energy. This indicates that if one quantizes semiclassically the orbits around these two fixed points, one would get two identical sets of quasi-energies. This explains the double degeneracy.

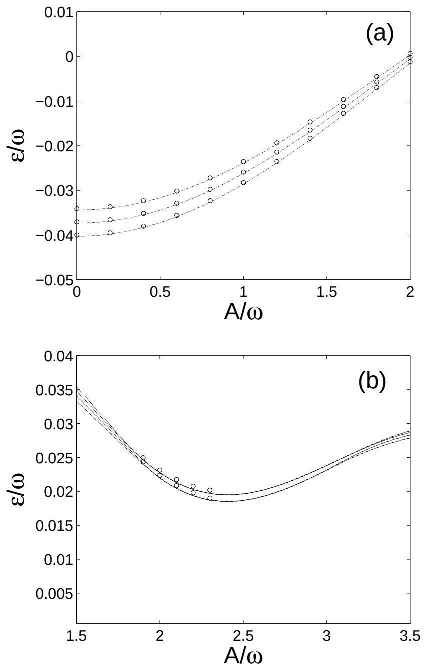

FIG. 7: Comparison between the quantum quasi-energy levels (solid lines) with $N = 40$ and semiclassical quasi-energy levels (open circles) at $c = 0.4, v = 1, \omega = 10$. (a) nondegenerate quasi-energy levels; (b) degenerate quasi-energy levels. For clarity, we have only plotted a portion of the quasi-energy levels.

IV. CONCLUSIONS

To summarize, we have studied the quasi-energies and Floquet states of two weakly coupled Bose-Einstein condensates subject to a periodic driving. Both the mean-field model and the second quantized model are used. A triangular structure was found in both mean-field quasi-energy levels and quantum quasi-energy levels. Moreover, we have revealed that the quantum quasi-energy levels are bound by their mean-field counterparts and we have explained it with semiclassical quantization. In addition, by looking into the Floquet states, we have found that the triangle in the quasi-energies is related a localization phenomenon which we call nonlinear coherent destruction of tunneling (NCDT).

Acknowledgments

We thank the helpful discussion with Jie Liu. This work is supported by the "BaiRen" program of Chinese Academy of Sciences, the NSF of China (10504040), and the 973 project of China(2005CB724500,2006CB921400).

[1] M. Grifoni, and P.Hänggi, Phys. Rep. **304**, 229(1998).
[2] F. Dalfovo, S. Griorgini, L.P.Pitaevskii, and S. Stringari, Rev. Mod. Phys. **71**, 463(1999).
[3] A. J. Leggett, Rev. Mod. Phys. **73**, 307(2001).
[4] G.J. Milburn, J. Corney, E.M. Wright, and D.F. Walls, Phys. Rev. A **55**, 4318(1997); A. Smerzi, S. Fantoni, S. Giovanazzi, and S.R. Shenoy, Phys. Rev. Lett. **79**, 4950 (1997); S. Raghavan, A. Smerzi, and V. M. Kenkre, Phys. Rev. A **60**, R1787 (1999); S. Raghavan, A. Smerzi, S. Fantoni, and S. R. Shenoy, Phys. Rev. A **59**, 620 (1999).
[5] M. Anderlini, J. Sebby-Strabley, J. Kruse, J. V. Porto, and W. D. Phillips, J. Phys. B **39**, S199 (2006).
[6] M. Albiez, R. Gati, J. Fölling, S. Hunsmann, M. Cristiani, and M. K. Oberthaler, Phys. Rev. Lett. 95, 010402 (2005).
[7] S. Levy, E. Lahoud, I. Shomroni, and J. Steinhauer. Nature **449**, 579 (2007).
[8] B. Wu and Q. Niu, Phys. Rev. A **61**, 023402(2000).
[9] M. Cristiani, O. Morsch, J. H. Müller, D. Ciampini, and E. Arimondo. Phys. Rev. A **65**, 063612(2002).
[10] W. A. Lin and L. E. Ballentine, Phys. Rev. Lett. **65**, 2927 (1990).
[11] A. Peres, Phys. Rev. Lett. **67**, 158 (1991).
[12] I. Vorobeichik and N. Moiseyev, Phys. Rev. A, **59**, 2511 (1999).
[13] F. Grossmann, T. Dittrich, P. Jung, and P. Hanggi, Phys. Rev. Lett. **67**, 516 (1991); Z. Phys. B **84**, 315 (1991).
[14] F. Grossmann and P. Hanggi, Europhys. Lett. **18**, 571 (1992).
[15] D. H. Dunlap and V. M. Kenkre, Phys. Rev. B **34**, 3625 (1986); Phys. Lett. A **127**, 438 (1988).
[16] R. Bavli and H. Metiu, Phys. Rev. Lett. **69**, 1986 (1992).
[17] M. Steinberg and U. Peskin, J. Appl. Phys. **85**, 270 (1999).
[18] M. Holthaus, Phys. Rev. Lett. 69, 351 (1992).
[19] G. S. Agarwal and W. Harshawardhan, Phys. Rev. A **50**, R4465 (1994).
[20] K. W. Madison, M. C. Fischer, R. B. Diener, Q. Niu, and M. G. Raizen, Phys. Rev. Lett. **81**, 5093 (1998);
[21] V. M. Kenkre and S. Raghavan, J. Opt. B: Quantum Semiclassical Opt. **2**, 686 (2000); S. Raghavan, V. M. Kenkre, D. H. Dunlap, A. R. Bishop, and M. I. Salkola, Phys. Rev. A **54**, R1781 (1996).
[22] H. L. Haroutyunyan and G. Nienhuis, Phys. Rev. A **64**, 033424 (2001).
[23] M. A. Jivulescu and E. Papp, J. Phys.: Condens. Matter **18**, 6853 (2006).
[24] M. Holthaus, Phys. Rev. A. **64**, 011601(R)(2001); A. Eckardt, T. Jinasundera, C. Weiss, and M. Holthaus Phys. Rev. Lett. **95**, 200401(2005); T. Jinasundera, C. Weiss, and M. Holthaus, Chem. Phys. **322**, 118(2006); M. Holthaus and S. Stenholm, Eur. Phys. J. B **20**, 451 (2001).
[25] Guan-Fang Wang, Li-Bin Fu, and Jie Liu, Phys. Rev. A. **73**, 013619(2006).
[26] B.-Y. Ou, X.-G. Zhao, J. Liu, S.-G. Chen, Phys. Lett. A.

291, 17(2001).
[27] N. Tsukada, M. Gotoda, Y. Nomura, and T. Isu, Phys. Rev. A. **59**, 3862(1999).
[28] Q. Xie and W. Hai, Phys. Rev. A. **75**, 015603 (2007).
[29] C. E. Creffield, Phys. Rev. A. **75**, 031607(R)(2007).
[30] F. Kh. Abdullaev and R. A. Kraenkel, Phys. Rev. A **62**, 023613(2000).
[31] Xiaobing Luo, Qiongtao Xie, and Biao Wu, Phys. Rev. A **76**, 051802(R) (2007).
[32] Qiongtao Xie, Xiaobing Luo, and Biao Wu, preprint.
[33] H. Lignier, C. Sias, D. Ciampini, Y. Singh, A. Zenesini, O. Morsch, and E. Arimondo, Phys. Rev. Lett. **99**, 220403 (2007).
[34] B. Wu and Q. Niu, New J. Phys. **5**, 104(2003).
[35] Y. Kayanuma, Phys. Rev. A **50**, 843 (1994); Yosuke Kayanuma and Yoshihiko Mizumoto, Phys. Rev. A **62**, 061401(R)(2000).
[36] Z. P. Karkuszewski, K. Sacha, and A. Smerzi, Eur. Phys. J. D. **21**, 251(2002).
[37] B. Wu, J. Liu, Phys. Rev. Lett. **96**, 020405(2006).
[38] H. Sambe, Phys. Rev. A **7**, 2203(1973).
[39] J. H. Shirley, Phys. Rev. **138**, B979 (1965).
[40] L.G. Yaffe, Rev. Mod. Phys. 54, 407 (1982); Wei-Min Zhang, Da Hsuan Feng, and R. Gilmore, Rev.Mod. Phys. 62, 867 (1990).
[41] R. Shankar, Phys. Rev. Lett. **45**, 1088 (1980).
[42] A. Garg and M. Stone, Phys. Rev. Lett. **92**, 010401 (2004).
[43] E. M. Graefe and H. J. Korsch, Phys. Rev. A **76**, 032116 (2007).
[44] H. P. Breuer and M. Holthaus, Ann. Phys.(N.Y.) **211**, 249(1991).
[45] F. Bensch, H. J. Korsch, B. Mirbach and N. Ben-Tal, J. Phys. A: Math. Gen. **25**, 6761(1992); B. Mirbach and H. J. Korsch. J. Phys. A: Math. Gen. **27**, 6579(1994).